RESEARCHERID
THOMSON REUTERS

[Shaif* *et al.*, 6(10): October, 2017]
IC™ Value: 3.00

ISSN: 2277-9655
Impact Factor: 4.116
CODEN: IJESS7

IJESRT

INTERNATIONAL JOURNAL OF ENGINEERING SCIENCES & RESEARCH TECHNOLOGY

STUDY AND ANALYSIS OF SANDWICH PANELS WITH FUNCTIONALLY GRADED CORE

Mohd. Shaif[*1], Er.Niklesh N. Singh[2] & Dr. Prabhat Kumar Sinha[3]

[*1]M. Tech. Scholar, Dept. of Mechanical Engineering, SHUATS, Allahabad, U.P., India

[2&3]Assistant Professor, Dept. of Mechanical Engineering, SHUATS Allahabad, U.P., India

DOI: 10.5281/zenodo.1036418

ABSTRACT

This study presents different analytical and finite element models for sandwich structures with functionally graded core. The trade-off between weight and stiffness as well as a comparison between these structures and sandwich structures with homogenous core is also presented. The problem of low-velocity impact between a sandwich structure with functionally graded core and a rigid spherical indentor is solved. A few advantages and disadvantages of these types of structure are presented. Although sandwich structure offer advantages over other types of structures, it is important to develop new types of materials in order to obtain the absolute minimum weight for given conditions (e.g., structural geometry and loadings). One alternative is represented by functionally graded materials (defined as materials with properties that vary with location within the material in order to optimize a prescribed function). With the new developments in manufacturing methods these materials can be used for a large number of applications ranging from implant teeth to rocket frames

KEYWORDS: Sandwich panels, Functionally graded materials, FG soft-core, Sandwich plate, FGM.

I. INTRODUCTION

A sandwich structure consists of two thin, stiff, and strong face sheets connected by a thick, light and low-modulus core using adhesive joints in order to obtain very efficient lightweight structure. In most of the cases the faces carry the loading, both in-plane and bending, while the core resists transverse shear loads. A sandwich operates in the same way as an I-beam with the difference that the core of a sandwich is of a different material and is stretched out as a continuous support for the face sheets. The main advantage of a sandwich structure is its exceptionally high flexural stiffness-to-weight ratio compared to other architectures. As a consequence, sandwich construction results in lower lateral deformations, higher buckling resistance, and higher natural frequencies than do other structures. Thus, for a given set of mechanical and environmental loads, sandwich construction often results in a lower structural weight than do other configurations. Few of the drawbacks of sandwich structures are: manufacturing methods, quality control and joining difficulties. Laminated composite plate with reinforced fibre has lighter weight and higher ratios of strength and stiffness to weight, therefore it has been widely applied to many aeronautical and astronautical structures as well as architecture and light industry products. With the quality improvement and occurrence of many new kinds of composite materials, their applications have become more and more extensive. However, laminated composite structures are weak in withstanding shock and likely to be aging, and some damage, such as delamination and crack, may often occur during their usage. These disadvantages will lead to a deterioration of the performance and even failure of the composite materials. Any damage in a composite structure always starts from a very tiny extent and gradually cumulates to some degree that can arouse people's attention. However, when such damage in a structure reaches a notable level, a serious accident will be induced. Obviously, the early discovery of incipient damage and the continuously monitoring for the growth and location of damage are the most essential issues in automatic damage inspection of in-service composite structures. Recently, great attention has been paid to the concept of smart material structures. A smart structure is the one that can sense its internal state and the external environment, and based on the information gained responds in a manner that can fulfill its functional requirements. The primary advantage of smart structure technology is the potential cost saving due to adopting condition-based maintenance strategies and the prospective structural life extension that may be achieved through damage repairing. The online detection of incipient damage for composite structures is relatively new concepts that are being developed globally to provide more safe, reliable and affordable composite structures.

ISSN: 2277-9655
Impact Factor: 4.116
CODEN: IJESS7

How to identify damage using the information obtained from a damaged composite structure is one of the most pivotal research objectives. Various structural damage causes the variation of structural mechanical characteristics, and this property has been extensively used for structural damage detection some comprehensive literature reviews about vibration-based structural damage identification. Many strategies, such as modal frequency approach , transmittance functions approach, resonance approach , mechanical impedance approach , comparing the piezoelectric conductance signature with the baseline signature of the healthy state , and wavelet-based approach , have been used to detect structural damage. However, in most of these approaches attention is mainly concentrated on whether damage has occurred in the structures. Only a little attention has been paid to the lowest extent of structural damage that can be detected. The satisfactory solution of the posed issue depends on whether the tiny delamination damage can be expressed in the dynamic model of a composite structure. Nowadays, the development of advanced micro-mechanics of composite damage has provided the feasibility to express tiny damage in the dynamic model of various composite structures , and many micro-mechanics models of composite damage have been developed, such as damage model of tensor inner variables, damage model of generalized elasticity, meso-scale damage model, and models of micro-crack damage and crack extension . Therefore, based on the dynamic model that can indicate tiny damage in any position of a composite structure, structural dynamic responses due to various possible tiny damage can be numerically simulated. However, literature on this topic has not been found so far. In this study, five piezoelectric patches, one acts as the actuator and the other four as the sensors, are embedded in a laminated composite plate for obtaining the dynamic responses of the plate, and the dynamic model of the plate is established using FEM and micromechanics theory of composite damage. The reliability of this model is verified using experiments. According to the energy distribution of the decomposed structural dynamic responses using wavelet packet analysis in various frequency bands, the index vector for structural damage detection is extracted. It is shown that a very tiny delamination damage area in a laminated composite plate can be well identified when the structure is actuated using the excitation signal with ample frequency composition. The numerical results show that it is possible to detect the damage of a delamination area less than 0.13% of the total area of the composite plate through a comparison of energy spectra of the multiorder wavelet decomposition signals of structural dynamic responses. While using comparison of the vibration modal parameters (natural frequency, modal damping and mode shape, etc.) with the baseline data of an intact structure, it can only detect delamination damage of more than 5–10% of the length of a composite beam . This shows that the method developed in this study is much more sensitive than the existing ones. the feature proxy for structural delamination damage is extracted from vibration response data of a structure with the known delamination damage including its location and size, so the corresponding relationships between the feature proxy and the real delamination damage parameters can be established by using the data obtained according to the corresponding relationships as database or the train samples of neural network, to detect the location and size of the unknown delamination damage based on the vibration response data of a structure with such unknown delamination damage. This is because the on-line vibration response data can be easily measured. the first step study for delamination detection. The main contents include data acquisition of vibration response using the established structural dynamics model, and the extraction of the feature proxy for different locations and sizes of delamination damage using wavelet transform of structural vibration responses.

II. RESEARCH OBJECTIVES

1. Develop analytical models for sandwich structures with functionally graded core.
2. Solve contact and impact problems involving sandwich structures with FG core and compare the trade-off between using a functionally graded core as opposed to the conventional sandwich design.
3. Compare the trade-off between the total mass and stiffness in functionally graded materials and homogenous materials by solving optimizations problems.

BuketOkutan Baba (2016), Analyzed the perforation energy and failure modes of curved sandwich composites with layer wise graded cores were experimentally. Three types of foam were used for flat and curved sandwich composites with layered cores. A series of six different core layer arrangements. They observed the contact forces, displacements and corresponding perforation energies of square panels were measured and failure modes after perforation. They obtained the results that the perforation energies of the sandwich panels were dependent on various geometrical and material parameters. The perforation energies of the curved panels with single type foam were increased compared to similar flat panels, whereas panels with graded foam behaved differently due to the foam layer arrangements.**Xinwei Wang ZhangxianYuan.(2016),** proposed to accurately analyze the static behavior of sandwich panels with FG soft-cores. Two combinations of boundary conditions and three types of loading were considered. Due to the severe transverse variations in the material properties and the

ISSN: 2277-9655
Impact Factor: 4.116
CODEN: IJESS7

discontinuity of the first order derivative of material parameters at the middle plane for point discrete methods and was solved by the weak form quadrature element method (QEM). They obtained the results which were verified with ABAQUS data by using very fine meshes &numerical results were presented to investigate effects of the power-law exponent of the material prosperities with variation, boundary conditions **Shiqiangli,xinli,et.ol (2017)** Analyzed the Sandwich panels with triple layered graded honeycomb cores were tested under blast loading, The structural deformation modes were classified into three types and the core layer deformation was divided into three regions. For the same value of impulse, a localized impulse led to severely localized deformation mode A relatively evenly distributed impulse resulted in largely global bending deformation. They concluded that under the same loading, graded panels with the core of the largest relative density placed near the impact face suffered a smaller deflection than the panels with uniform core. **Jacob M.Quintana Todd M.Mower (2017),** Analyzed Sandwich panels constructed with carbon-fiber facesheets and graphitic-foam cores could provide a viable solution for optical benches which required high stiffness and thermal stability. They presented that the panels exhibit lower susceptibility to thermal distortion than sandwich panels constructed with traditional honeycomb cores or monolithic plates of materials having low thermal Investigated the, thermomechanical bending analysis of functionally graded material (FGM) sandwich plates was performed by using a four-variable refined plate theory. A new type of FGM sandwich plates, namely, both FGM face sheets and FGM hard core were considered. Containing only four unknown functions, the governing equations were deduced based on the principle of virtual work and then these equations were solved via Navier approach. They obtained the analytical solutions to predict the deflections and stresses of simply supported FGM sandwich plates.

LinJing FeiYang LongmaoZhao(2017), Presented that the perforation resistance capability of clamped square sandwich panels with layered gradient metallic foam cores subjected to the hemispherical-nosed projectile impact was investigated numerically. They presented the simulation results which indicate the layered-gradient sandwich had the worst perforation resistance and energy absorption capability. They found that the ungraded sandwich panel and the monolithic plate was the best.**A.Aliyari ParandA.Alibeigloo (2017),** Presented that the elasticity solution for static and free vibration analysis of sandwich cylindrical shell with functionally graded (FG) core and viscoelastic interface. Variation of Young's Module and material density of FGM core layer were obey the power-law of radial coordinate with the Poisson's ratio which holds to constant. Time-dependent behavior was determined by solving first-order differential equation of sliding displacement at the viscoelastic interfaces. They presented the numerical results were computed and compared with the reported results to validate the present approach. They found effects of solid, elastic interfaces, different boundary conditions, time and mid radius to thickness ratio on the bending and vibration behaviour of the sandwich shell.**S.Jedari Salami (2017),** Analyzed the response of sandwich beam with carbon nanotube reinforced composite (CNTRC) face sheets and soft core subjected to the action of an impacting mass based on the Extended High Order Sandwich Panel Theory (EHSAPT). Distribution of fibers through the thickness of the face sheets could be uniform or functionally graded (FG). Contact force between the impactor and the beam was obtained using the conventional Hertz law. The field equations were derived via the Ritz based applied to the total energy of the system. They obtained the solution in the time domain by implementing the well-known Runge–Kutta method. After examining the validity of the present solution, the effects of distribution of Carbon Nanotubes (CNTs), nanotube volume fraction, core-to-face sheet thickness ratio, initial velocity of the impactor and the impactor mass. They concluded that the highest peak contact force and the lowest indentation of the top face sheet belong to the sandwich beam with distribution of face sheet.**José S.MoitaAurélio L.AraújoCristóvão M.Mota SoaresCarlos A.Mota Soares (2017),** Presented a finite element model which was developed for vibration analysis of pure functionally graded material (FGM) structures and for passive damped sandwich structures with a soft viscoelastic core between the FGM layers were modeled by using the classical plate theory and the core was modeled by using Reddy's third-order shear deformation theory. The finite element was obtained by using specific assumptions on the displacement continuity at the interfaces between layers. They conducted the study to the time domain steady state harmonic motion for both analyses the finite element code. Although FGMs are highly heterogeneous, it will be useful to idealize them as continua with properties that change smoothly with respect to spatial coordinates. This will enable closed-form solutions for some fundamental solid mechanics problems, and will aid the development of finite element models for structures made of FGMs. This chapter investigates different analytical models available in literature for a sandwich beam and applies them to a sandwich beam with functionally graded core. In the first two sections, the governing equations for sandwich structures with FG cores are solved for two types of core Young Modulus by two different methods: exact solutions are presented for the exponential variation of core Young Modulus and a combination of Fourier series and Galerkin method for a polynomial variation of core Young Modulus. Those methods are compared with two

ISSN: 2277-9655
Impact Factor: 4.116
CODEN: IJESS7

equivalent single-layer theories based on assumed displacements, a higher-order theory and a finite-element analysis. A very good agreement among the Fourier series-Galerkin method, the higher-order theory and the finite-element analysis is found.

Exact Method for Sandwich Structures with Functionally Graded Core

Venkataraman and Sankar (2001) derived an elasticity solution for stresses in a sandwich beam with a functionally graded core. They used Euler-Bernoulli beam theory for analysis of face sheets and plane elasticity equations for the core. In the present work, the solution of the sandwich problem was improved by using elasticity equation for face sheets also.

The dimensions of the sandwich beam are shown in Figure 2.1.The length of the beam is L, the core thickness is h and the face sheet thicknesses are h_f. The beam is divided into 4 parts or elements: the top face sheet, top half of the core, bottom half of the core and the bottom face sheet.

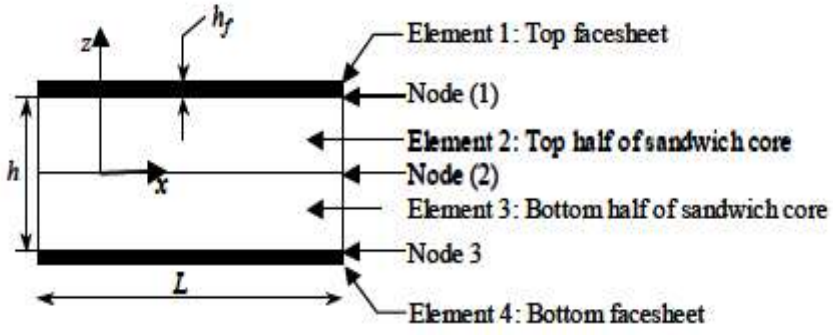

Figure 2.1: Sandwich beam with functionally graded core with schematic of the analysis elements.

In general, this model can be applied for sandwich structures with core and face sheets orthotropic materials at every point and the principal material directions coincide with the x and z-axes.Consequently, the constitutive relations for each layer are:

$$\begin{Bmatrix}\sigma_{xx}\\ \sigma_{xx}\\ \tau_{xz}\end{Bmatrix}_i = \begin{bmatrix}C_{11} & C_{13} & 0\\ C_{13} & C_{33} & 0\\ 0 & 0 & C_{55}\end{bmatrix}_i \begin{Bmatrix}\varepsilon_{xx}\\ \varepsilon_{xx}\\ \gamma_{xz}\end{Bmatrix}_i, \text{ for } i^{th} \text{ element } i = 1,2,3,4$$

Or

$$\{\sigma\} = [C(z)]\{\varepsilon\}$$

The face sheets are assumed to be homogeneous and isotropic. The core is functionally graded but symmetric about the mid-plane given by $z=0$. The elastic coefficients (c_{ij}) of the core are assumed to vary according to:

$$C_{ij} = C^{o}_{ije}$$

This exponential variation of elastic stiffness coefficients allows exact elasticity solution.

The tractions and displacements at the interface between each element are shown in Figure 2.2. Each element has its own coordinate systems. The coordinate systems of each element are chosen at the interface because displacements and traction compatibility between elements will have to be enforced at these nodes.

ISSN: 2277-9655
Impact Factor: 4.116
CODEN: IJESS7

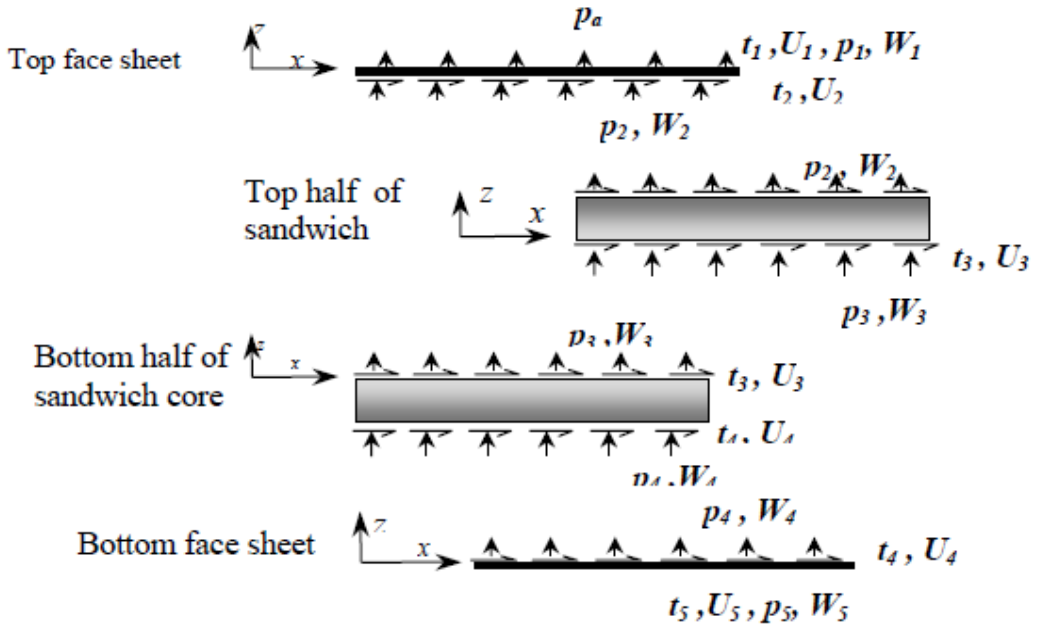

Figure 2.2: Traction forces and displacements at the interfaces of each element in the FGM sandwich beam

The governing equations are formulated separately for each element, and compatibility of displacements and continuity of tractions are enforced at each interface (node) to obtain the displacement and stress field in the sandwich beam. This procedure is analogous to assembling element stiffness matrices to obtain global stiffness matrix in finite element analysis.

The top face sheet is subjected to normal tractions such that:

$$\sigma_{xx}(x,0) = p_a \sin(\xi x)$$

Where

$$\xi = \frac{n\pi}{L}, \text{ n} = 1,3,5,\ldots.$$

and p_a is known. Since n is assumed to be odd, the loading is symmetric about the center of the beam. The loading given by equation (1.20) is of practical significance because any arbitrary loading can be expressed as a Fourier series involving terms of the same type.

The displacement field for each layer is assumed of the form:

$$u_i(x,z) = U_i(z)\cos(\xi x)$$

i = 1,2,3,4

$$w_i(x,z) = W_i(z)\sin(\xi x)$$

where u is horizontal displacement and w is vertical displacement and where it is assumed that:

$(U_i, W_i) = (a_i, b_i)\exp(\alpha_i z)$

where a_i, b_i, α_i are constants to be determined.

In order to satisfy equilibrium the contributions of the different tractions at each interface should sum to zero. Enforcing the force balance and the compatibility of force and displacements at the interfaces enables us to assemble the stiffness matrices of the four elements to obtain a global stiffness matrix K:

ISSN: 2277-9655
Impact Factor: 4.116
CODEN: IJESS7

$$[\boldsymbol{K}]\{U_1\ W_1\ U_2\ W_2\ U_3\ W_3\ U_4\ W_4\ U_5\ W_5\} = \{0\ p_a\ 0\ 0\ 0\ 0\ 0\ 0\ 0\ 0\}$$

where ***K*** is the global stiffness matrix, a summation of the stiffness matrices for each element. The displacements $U_1, W_1 \ldots W_5$, are obtained by solving (1.24). The obtained displacement field along with the constitutive relations is used to obtain the stress field in each element.

Fourier – Galerkin Method for Sandwich Structures with Functionally Graded Core

Zhu and Sankar (2004) derived an analytical model for a FG beam with Young's modulus expressed as a polynomial in thickness coordinate using a combined Fourier SeriesGalerkin method. In the present work, the model is applied to a sandwich beam with FG core. The geometry (Figure 2.1), the load (1.20), and the constitutive relations (1.17) are the same as in previous model.

In this section, a brief description of the procedures to obtain the stiffness matrix of top half of the core is provided. The derivation of stiffness matrices of other elements follows the same procedures.

The differential equations of equilibrium for the top half of the core are:

$$\frac{\partial \sigma_{xx}}{\partial x} + \frac{\partial \tau_{xz}}{\partial z} = 0$$

$$\frac{\partial \tau_{xz}}{\partial x} + \frac{\partial \sigma_{zz}}{\partial z} = 0$$

The variation of Young's modulus, *E* in the thickness direction is given by a polynomial in *z*. e.g.,

$$E(z) = E_0\left(a_1\left(\frac{z}{h}\right)^4 + a_2\left(\frac{z}{h}\right)^3 + a_3\left(\frac{z}{h}\right)^2 + a_4\left(\frac{z}{h}\right) + 1\right)$$

where E_0 is the Young's modulus at $z=0$ anda_1, a_2, a_3 and a_4 are material constants. The thickness in *y* direction is large and plain strain assumption can be used. The elasticity matrix [***C***] is related to the material constants by:

$$[C] = \frac{E(z)}{(1+v)(1-2v)}\begin{pmatrix} 1-v & v & 0 \\ v & 1-v & 0 \\ 0 & 0 & \frac{1-2v}{2} \end{pmatrix}$$

The following assumptions are made for displacements:

$u(x,z) = U(z)\cos\xi x$

$w(x,z) = W(z)\sin\xi x$

Substituting equation (1.28) into (1.27), the following constitutive relation is obtained:

$$\begin{pmatrix}\sigma_{xx}\\ \sigma_{zz}\\ \tau_{xz}\end{pmatrix} = \begin{pmatrix} c_{11} & c_{13} & 0 \\ c_{13} & c_{33} & 0 \\ 0 & 0 & G \end{pmatrix}\begin{pmatrix} -\xi U\sin\xi x \\ W'\sin\xi x \\ U' + \xi W\cos\xi x \end{pmatrix}$$

A prime (′) after a variable denotes differentiation with respect to *z*. Boundary conditions of the beam at $x=0$ and $x=L$ are $w(0,z)=w(L,z)=0$, and $\sigma_{xx}(0,z) = \sigma_{xx}(L,z) = 0$, which corresponds to simple support conditions in the context of beam theory. Equations (1.29) can be written as:

$$\begin{pmatrix}\sigma_{xx}\\ \sigma_{zz}\end{pmatrix} = \begin{pmatrix}S_x\\ S_z\end{pmatrix}\sin\xi x$$

$$\tau_{xz} = T_Z\cos\xi x$$

ISSN: 2277-9655
Impact Factor: 4.116
CODEN: IJESS7

Where

$$\begin{pmatrix} S_x \\ S_z \end{pmatrix} = \begin{pmatrix} c_{11} & c_{13} \\ c_{13} & c_{33} \end{pmatrix} \begin{pmatrix} -\xi U \\ W' \end{pmatrix}$$

$$T_z = G(U' + \xi W)$$

Substituting for $\sigma_{xx}, \sigma_{zz}, \tau_{xz}$ from equations (1.31) into equilibrium equations (1.25), a set of ordinary differential equations in $U(z)$ and *W(z)* are obtained:

$$\xi S_x + T_Z' = 0$$
$$S_Z' - T_Z \xi = 0$$

In order to solve equations (1.32) the Galerkin Method is employed: solutions in the form of polynomials in *z* are assumed:

$$\mathrm{U}(z) c_1 \emptyset_1(z) + c_2 \emptyset_2(z) + c_3 \emptyset_3(z) + c_4 \emptyset_4(z) + c_5 \emptyset_5(z)$$
$$\mathrm{W}(z) b_1 \emptyset_1(z) + b_2 \emptyset_2(z) + b_3 \emptyset_3(z) + b_4 \emptyset_4(z) + b_5 \emptyset_5(z)$$

where φs are basis functions, and *b*'s and *c*'s are coefficients to be determined. For simplicity *1*, *z*, z^2, z^3, z^4 are chosen as basis functions:

$$\emptyset_1(z) = 1; \quad \emptyset_2(z) = z; \quad \emptyset_3(z) = z^2;$$
$$\emptyset_4(z) = z^3; \quad \emptyset_5(z) = z^4$$

Substituting the approximate solution in the governing differential equations, the residuals are obtained. The residuals are minimized by equating their weighted averages to zero:

$$\int_0^h (\xi S_x + T_z') \emptyset_i(z)\, dz = 0, \qquad \text{i = 1,5}$$

$$\int_0^h (S_z' - T_Z \xi) \emptyset_I(z)\, dz = 0 \qquad \text{i = 1,5}$$

Using integration by parts (1.35) can be rewritten as:

$$\int_0^h \emptyset_1 \xi S_X\, dz + T_z(h)\emptyset_i(h) - T_z(0)\emptyset_i(0) - \int_0^h T_z \emptyset_i' dz = 0$$
$$\int_0^h S_z \emptyset_i' dz + \int_0^h T_z \xi \emptyset_i\, dz - \left(S_z(h)\emptyset_i(h) - S_z(0)\emptyset_i(0)\right) = 0, \qquad \text{i =1,5}$$

Substituting for $S_X(z), S_z(z)$ and $T_z(z)$ from equations (1.31) into (1.36) and using the approximate solution for *U(z)* and *W(z)* in (1.33) it is obtained:

$$\begin{pmatrix} K_{ij}^{(1)} & K_{ij}^{(2)} \\ K_{ij}^{(3)} & K_{ij}^{(4)} \end{pmatrix} \begin{pmatrix} b \\ c \end{pmatrix} = \begin{pmatrix} f_i^{(1)} \\ f_i^{(2)} \end{pmatrix}$$

Or

$$[\boldsymbol{K}] \begin{pmatrix} \boldsymbol{b} \\ \boldsymbol{c} \end{pmatrix} = \begin{pmatrix} \boldsymbol{f_i}^{(1)} \\ \boldsymbol{f_i}^{(2)} \end{pmatrix}$$

where:

$$K_{ij}^{(1)} = \xi \int_0^h c_{13} \emptyset_i \emptyset_j' dz - \xi \int_0^h G \emptyset_i' \emptyset_j\, dz$$

$$k_{ij}^{(2)} = -\int_0^h G \emptyset_i' \emptyset_j' dz - \xi^2 \int_0^h c_{11} \emptyset_i \emptyset_j\, dz$$
$$K_{ij}^{(3)} = -\xi^2 \int_0^h G \emptyset_i \emptyset_j\, dz - \int_0^h c_{33} \emptyset_i' \emptyset_j' dz \qquad \text{i = 1,5}$$

ISSN: 2277-9655
Impact Factor: 4.116
CODEN: IJESS7

$$K_{ij}^{(4)} = \xi \int_0^h c_{13}\emptyset_i'\emptyset_j\, dz - \xi\int_0^h G\emptyset_i\emptyset_j'\, dz$$

$$f_i^{(1)} = \emptyset_i(0)T_z(0) - \emptyset_i(h)T_Z(h)$$
$$f_i^{(2)} = \emptyset_i(0)S_z(0) - \emptyset_i(h)S_z(h)$$

$$\begin{pmatrix} b \\ c \end{pmatrix} = (b_1\ \ b_2\ \ b_3\ \ b_4\ \ b_5\ \ c_1\ \ c_2\ \ c_3\ \ c_4\ \ c_5)$$

Let U_2, W_2, U_3 and W_3 be the displacements at top and bottom surface of top half of the element (top half of the core). Evaluating the expressions for $U(z)$ and $W(z)$ at the top and bottom surfaces and equating them to the surface displacements results in the expression:

$$\begin{pmatrix} U_2 \\ W_2 \\ U_3 \\ W_3 \end{pmatrix} = \begin{pmatrix} 0 & 0 & 0 & 0 & 0 & 1 & h & h^2 & h^3 & h^4 \\ 1 & h & h^2 & h^3 & h^4 & 0 & 0 & 0 & 0 & 0 \\ 0 & 0 & 0 & 0 & 0 & 1 & 0 & 0 & 0 & 0 \\ 1 & 0 & 0 & 0 & 0 & 0 & 0 & 0 & 0 & 0 \end{pmatrix} \begin{pmatrix} b \\ c \end{pmatrix}$$

This can be compactly expressed as:

$$\begin{pmatrix} U_2 \\ W_2 \\ U_3 \\ W_3 \end{pmatrix} = [\boldsymbol{A}] \begin{pmatrix} b_1 \\ \vdots \\ c_5 \end{pmatrix}$$

The tractions T_2, P_2, T_3 and P_3 acting on the surface can be related to the functions f_i as follows:

$$\begin{pmatrix} f_1^{(1)} \\ f_2^{(1)} \\ f_3^{(1)} \\ f_4^{(1)} \\ f_4^{(1)} \\ f_1^{(2)} \\ f_2^{(2)} \\ f_3^{(2)} \\ f_4^{(2)} \\ f_5^{(2)} \end{pmatrix} = \begin{bmatrix} -\phi_1(h) & 0 & \phi_1(0) & 0 \\ -\phi_2(h) & 0 & \phi_2(0) & 0 \\ -\phi_3(h) & 0 & \phi_3(0) & 0 \\ -\phi_4(h) & 0 & \phi_4(0) & 0 \\ -\phi_5(h) & 0 & \phi_5(0) & 0 \\ 0 & -\phi_1(h) & 0 & \phi_1(0) \\ 0 & -\phi_2(h) & 0 & \phi_2(0) \\ 0 & -\phi_3(h) & 0 & \phi_3(0) \\ 0 & -\phi_4(h) & 0 & \phi_4(0) \\ 0 & -\phi_5(h) & 0 & \phi_5(0) \end{bmatrix} \begin{pmatrix} T_2 \\ S_2 \\ T_3 \\ S_3 \end{pmatrix}$$

or

$$\begin{pmatrix} f_1^{(1)} \\ \vdots \\ f_5^{(2)} \end{pmatrix} = [\boldsymbol{B}] \begin{pmatrix} \boldsymbol{T_2} \\ \boldsymbol{S_2} \\ \boldsymbol{T_3} \\ \boldsymbol{S_3} \end{pmatrix}$$

From (1.37), (1.42) and (1.44) follows:

$$\begin{pmatrix} U_2 \\ W_2 \\ U_3 \\ W_3 \end{pmatrix} = [\mathbf{A}][\mathbf{K}]^{-1}[\mathbf{B}] \begin{pmatrix} T_1 \\ S_1 \\ T_2 \\ S_2 \end{pmatrix} = [\mathbf{K}^*] \begin{pmatrix} T_1 \\ S_1 \\ T_2 \\ S_2 \end{pmatrix}$$

ISSN: 2277-9655
Impact Factor: 4.116
CODEN: IJESS7

Finally, the stiffness matrix of the top half of the FGM core $[S^{(2)}]$ that relates the surface tractions to the surface displacements is obtained as:

$$\begin{pmatrix} T_1 \\ S_1 \\ T_2 \\ S_2 \end{pmatrix} = \left[\mathbf{K}^*\right]^{-1} \begin{pmatrix} U_2 \\ W_2 \\ U_3 \\ W_3 \end{pmatrix} = \left[\mathbf{S}^{(2)}\right] \begin{pmatrix} U_2 \\ W_2 \\ U_3 \\ W_3 \end{pmatrix}$$

In order to satisfy equilibrium, the contributions of the different tractions at each interface should sum to zero. Enforcing the balance and the compatibility of force and displacements at the interfaces enables us to assemble the stiffness matrices of the four elements to obtain a global stiffness matrix [***S***]:

$$[\boldsymbol{S}][U_1 \ W_1 \ U_2 \ W_2 \ U_3 \ W_3 \ U_4 \ W_4 \ U_5 \ W_5] =$$

$$[0 \ p_a \ 0 \ 0 \ 0 \ 0 \ 0 \ 0 \ 0 \ 0]$$

The displacements $U_1, W_1 \ldots W_5$, are obtained by solving equation (1.47). The displacement field along with the constitutive relations is used to obtain the stress field in each element.

III. RESULTS

1. Maximum normal and shear strains for a given impact energy of 282 J. FG denotes functionally graded core. The % reduction in strain in FG cores is with respect to the maximum strain in uniform core.

Core type	E_h/E_0	$F_{max}(N)$	ε_x		γ_{xz}	
			Maximum	% Reduction	Maximum	% Reduction
Uniform	1	5.45×10^4	0.0300	–	0.0978	–
FG, Symmetric	5	7.03×10^4	0.0257	14.3	0.0830	0.0368
FG, Symmetric	10	7.89×10^4	0.0194	35.3	0.0700	28.4
FG, Asymmetric	5	7.39×10^4	0.0195	35.0	0.0500	48.9
FG, Asymmetric	10	7.39×10^4	0.0176	41.3	0.0368	62.3

2. Core thicknesses for different materials with same flexural stiffness, $D_{11}$and same global stiffness. H.C.: homogeneous core; S.C.: symmetric core, A.S.: asymmetric core.

ISSN: 2277-9655
Impact Factor: 4.116
CODEN: IJESS7

Core type	E_h/E_0	For constant D_{11}		For constant global stiffness	
		Core thickness, h (mm)	Global stiffness, k_s (MN/m)	Core thickness, h (mm)	Global stiffness, k_s (MN/m)
Uniform	1	20	5.5	20	5.65
Symmetric	5	12.58	4.4	14.44	5.65
Symmetric	10	10.08	3.67	12.88	5.65
Asymmetric	5	13.82	5.5	13.82	5.65
Asymmetric	10	11.28	4.78	12.32	5.65

3. Maximum normal and shear strains for a given impact energy of 282 J. FG denotes functionally graded core. The % change in strain in FG core is with respect to the maximum strain in uniform core.

Core type	E_h/E_0	F_{max} (N)	ε_x		γ_{xz}	
			Maximum	% Change	Maximum	% Change
Uniform	1	5.33×10^4	0.0125	-	0.0978	-
FG, Asymmetric	10	5.16×10^4	0.0135	+ 7.2	0.0368	- 23.32

IV. SUMMARY AND CONCLUSION

Based on two models found in the literature and based on different relations between relative density and elastic modulus, this chapter solves three optimization problems: the geometry of the sandwich panels is kept constant while the properties (Young's modulus and density) are changed such that to optimize the total mass and/or the flexural rigidity.

Choi and Sankar's (2005) linear relation between the relative density and Young's modulus is used to determine the FG asymmetric core and the uniform core parameters such as to obtain panels with the same mass and same flexural rigidity. The results of the impact problem prove that there is a significant reduction (approximately 24%) in the maximum shear strain corresponding to maximum impact load of FG asymmetric core compared with the uniform core maximum shear strain, while the maximum normal strains corresponding to maximum impact load are almost the same.

The second model is based on the quadratic relation between the relative density and Young's modulus derived by Gibson and Ashby (1997). The Young's modulus and the density were varied such as to obtain panels with same flexural rigidity or to obtain panels with the same total mass. The results of the impact analysis provided similar results for both problems: among the three sandwich panels (with homogeneous core, symmetric FG core and asymmetric FG core), the one with FG asymmetric core gives the smaller maximum shear strain corresponding to the maximum impact load The second model is based on the quadratic relation between the relative density and Young's modulus derived by Gibson and Ashby (1997). The Young's modulus and the density were varied such as to obtain panels with same flexural rigidity or to obtain panels with the same total mass. The results of the impact analysis provided similar results for both problems: among the three sandwich

ISSN: 2277-9655
Impact Factor: 4.116
CODEN: IJESS7

panels (with homogeneous core, symmetric FG core and asymmetric FG core), the one with FG asymmetric core gives the smaller maximum shear strain corresponding to the maximum impact load (approximately 27% less than the uniform core) while the difference in maximum normal strain corresponding to the maximum impact load is small. Also, when the properties are changed such as to obtain the same flexural rigidity, the sandwich panel with asymmetric FG core gives the smaller total mass.

These conclusions based on optimization studies emphasize again the superior capability of sandwich structures with FG cores over the sandwich structures with uniform cores.

V. REFERENCES

[1] A.Thamaraiselvan , A. Thanesh , K. Suresh ,& S. Palani "Design and Development of Reliable Integral Shaft Bearing for Water Pump in Automotive Engine to Reduce Assemble Time and Increase Production" Indian Journal of Science and Technology. (2016) vol 9, pages 221-229.
[2] Brian P. Graney & Ken Starry, "Rolling Element Bearing Analysis", from material Evaluation vol 70, pg 78-85, jan 2012
[3] Chen Guang. "Aero-engine structural design analysis" Beijing, beihang university, (2006) Page 114-159.
[4] JafarTakabi& M.M. Khonsari, "Experimental testing and thermal analysis of ball bearings", Department of Mechanical Engineering, 2508 Patrick Taylor Hall, Louisiana State University, Baton Rouge, LA 70803, United States, 19 October 2012.
[5] Jun sun, GuiChanglin, " Hydrodynamic lubrication analysis of journal bearing considering misalignment caused by shaft deformation," School of Mechanical and Automotive Engineering, Hefei University of Technology, May 2008.
[6] Laniado-Jacome Edwin," Numerical Model to Study of Contact Force in A Cylendrical Roller Bearing with Technical Mechanical Event Simulation", Mechanical Engineering department, carlos III University , Madrid, 28911, spain, March 2011.
[7] PrasannaSubbaraoBhamidipati, " FEA Analysis of Novel Design of Cylindrical Roller Bearing," mater thesis submitted in R.C.E, Affilated to Jawaharlal Nehru technological university Hydrabad, India may, 2009.
[8] Sriram Pattabhiraman, George Levesque. "Uncertainty analysis for rolling contact fatigue failure probability of silicon nitride ball bearings" International Journal of Solids and Structures (2010)Vol 47, Pages 2543–2553.
[9] Tang Zhaoping,Sun jianping," The Contact Analysis for Deep Groove Ball Bearing Based on ANSYS" Procedia Engineering (2011).
[10] Zhang Yongqi,Tan Qingchang,Zhang Kuo,Li Jiangang" Analysis of Stress and Strain of the Rolling Bearing by FEA method" International Conference on Applied Physics and Industrial Engineering(2012) vol 24 pages 19 – 24..

CITE AN ARTICLE

Shaif, M., Singh, N. N., & Sinha, P. K., Dr. (2017). STUDY AND ANALYSIS OF SANDWICH PANELS WITH FUNCTIONALLY GRADED CORE. *INTERNATIONAL JOURNAL OF ENGINEERING SCIENCES & RESEARCH TECHNOLOGY*, *6*(10), 534-544.